

The Lorenz Renormalization Conjecture

Björn Winckler*

May 4, 2018

Abstract

The renormalization paradigm for low-dimensional dynamical systems is that of hyperbolic horseshoe dynamics. Does this paradigm survive a transition to more physically relevant systems in higher dimensions? This article addresses this question in the context of Lorenz dynamics which originates in homoclinic bifurcations of flows in three dimensions and higher. A conjecture classifying the dynamics of the Lorenz renormalization operator is stated and supported with numerical evidence.

1 Introduction

Renormalization in low-dimensional dynamical systems is characterized by hyperbolic horseshoe dynamics with contraction within topological families and expansion otherwise. There are an abundance of low-dimensional systems which adhere to this paradigm, such as unimodal maps (Avila and Lyubich, 2011), critical circle maps (Yampolsky, 2003) and circle maps with breaks (Khanin and Teplinsky, 2013); as well as partial results for dissipative Hénon-like maps (De Carvalho et al., 2005), area-preserving maps (Eckmann et al., 1984; Gaidashev et al., 2016) and higher-dimensional analogs of unimodal maps (Collet et al., 1981). This research springs from the question: in what way does the renormalization paradigm need to be modified as its scope is expanded to include more physically relevant systems coming from flows and maps in higher dimensions?

We expect renormalization phenomena like universality to survive due to the fact that they have been measured in real physical systems (Maurer and Libchaber, 1979; Linsay, 1981), as first predicted to be possible by Couillet and Tresser (1978). Surprisingly, it was shown in Martens and Winckler (2017) that even in the one-dimensional setting of Lorenz maps, instability of renormalization is not only associated with changes in topology; the dynamics of the renormalization operator inside topological classes is not necessarily a contraction. This also has a fundamental impact on the question of rigidity as discussed in § 1.3.

*Department of Mathematics, Imperial College London, London SW7 2AZ, UK, bjorn.winckler@gmail.com. This project has received funding from the European Union's Horizon 2020 research and innovation programme under the Marie Skłodowska-Curie grant agreement No 743959.

The purpose of this article is to state a conjecture which classifies the dynamics of the Lorenz renormalization operator and to support this conjecture with numerical experiments. We hope that it will act as a focus for what should aim to be proven for these systems. More importantly, we wish to provide an indication of what kind of renormalization phenomena to expect as the field transitions towards physically relevant systems.

The article is organized into two sections. In this introduction we go over the necessary definitions and make several remarks along the way before stating the Lorenz Renormalization Conjecture in § 1.4. Having accomplished that, we go on to describe the numerical experiments performed to support the conjecture and include the results of these experiments. The source code, together with instructions on how to reproduce the results, are freely available online (Winckler, 2018).

1.1 Lorenz maps

Definition 1.1. Let $I = [l, r]$ be a closed interval. A **Lorenz map** f on I is a monotone increasing function which is continuous except at a **critical point**, $c \in (l, r)$, where it has a jump discontinuity, and $f(I \setminus \{c\}) \subset I$ (see figure 1).

The branches¹ $f_0 : [l, c] \rightarrow I$ and $f_1 : [c, r] \rightarrow I$ of f are assumed to satisfy: (i) $f_0(c) = r$ and $f_1(c) = l$, (ii) $f_k(x) = \phi_k(|c-x|^\alpha)$, for some **critical exponent** $\alpha > 0$, and C^2 -diffeomorphisms ϕ_k , $k = 0, 1$.

The **set of Lorenz maps** on $[0, 1]$ is denoted \mathcal{L} .

Convention. Unless the interval I in the above definition is mentioned, it is implicitly assumed to be the unit interval $[0, 1]$.

Remark 1.2. It bears pointing out that the critical point c is *not* fixed, but depends on the map f . Later on we will see that the critical point moves under renormalization. This is an essential feature of Lorenz maps which has very strong consequences on the dynamics and results in new renormalization phenomena not present in unimodal and circle dynamics (Martens and Winckler, 2017).

Remark 1.3. The second condition on the branches ensures that the behavior of f near the critical point is like that of the power map x^α near 0. This condition and the assumption $\alpha > 1$ leads to a well-defined renormalization theory.

Convention. The critical exponent $\alpha \in \mathbb{R}$ is fixed and $\alpha > 1$.

Remark 1.4. Lorenz maps were introduced by Guckenheimer and Williams (1979) in order to describe the dynamics of three-dimensional flows geometrically similar to the well-known Lorenz system (Lorenz, 1963). The flows they consider have a saddle with a one-dimensional unstable manifold which exhibits recurrent behavior. Their construction is to take a transversal section to the

¹Even though f is undefined at c , its branches continuously extend to c since f is bounded.

stable manifold and assume that the associated first-return map has an invariant foliation whose leaves are exponentially contracted. Taking a quotient over the leaves results in a one-dimensional map as described by definition 1.1.

In the above construction the critical exponent α naturally comes out as the absolute value of the ratio between two eigenvalues of the linearized flow at the singularity. In particular, it is important for Lorenz theory to be able to handle any real critical exponent $\alpha > 0$ (as opposed to unimodal theory where it may be possible to get away with saying something like “the critical exponent is generically two”). Guckenheimer and Williams (1979) considered $\alpha \in (0, 1)$; the first to investigate $\alpha > 1$ were Arneodo et al. (1981).

Remark 1.5. In more generality, Lorenz maps can be thought of as the underlying dynamical model for a large class of higher dimensional flows undergoing a homoclinic bifurcation. Hence there are very strong reasons why Lorenz dynamics needs to be further explored. We can only guess that this theory is still so largely underdeveloped, as compared to unimodal and circle dynamics, because of the fact that the holomorphic tools developed in these other theories are not suitable for adaptation to discontinuities and arbitrary real critical exponents. New ideas and tools are desperately needed!

Remark 1.6. There is a genuine problem relating to smoothness that needs mentioning. Even if the invariant foliation mentioned in remark 1.4 is smooth, the holonomy map need not be (Milnor, 1997; Hirsch et al., 1977). Hence, the associated Lorenz map need not have C^2 branches, regardless of how smooth the initial flow is. Without C^2 -smoothness the renormalization apparatus breaks down (Chandramouli et al., 2009). In transferring results about maps to flows this problem needs to be addressed.

1.2 Renormalization

Definition 1.7. Let $A_I : [0, 1] \rightarrow I$ denote the increasing affine map taking $[0, 1]$ onto I . The **rescaling** to $[0, 1]$ of $g : U \rightarrow V$ (synonymously, g **rescaled** to $[0, 1]$) is the map $G : [0, 1] \rightarrow [0, 1]$ defined by $G = A_V^{-1} \circ g \circ A_U$. In this situation we also conversely say that g is a rescaling of G .

Definition 1.8. A Lorenz map f is **renormalizable** iff there exist $n_0, n_1 \geq 2$ such that $I = [f^{n_1-1}(0), f^{n_0-1}(1)]$ is contained in $(0, 1)$ and contains c in its interior, and such that the first-return map to I is again a Lorenz map (on I); the first-return map rescaled to $[0, 1]$ is called a **renormalization** of f and the symbolic coding of its branches defines the **type** (or **combinatorics**), $w = (w_0, w_1)$, of the renormalization.² In this case we also say that f is **w-renormalizable** and call the rescaled first-return map a **w-renormalization**.

Definition 1.9. The type $w = (w_0, w_1)$ is said to be of **monotone combinatorics** if $w_0 = 011 \cdots 1$ and $w_1 = 100 \cdots 0$; more succinctly, it is also called **(a, b) -type**, where $a = |w_0| - 1$ and $b = |w_1| - 1$.

²Explicitly, let $I_k = I \cap [k, c)$ and define w_k to be the finite word on symbols $\{0, 1\}$ such that $f^j(I_k) \subset [w_k(j), c)$ for $j = 0, \dots, |w_k| - 1$ and $k = 0, 1$.

Remark 1.10. A Lorenz map may have more than one renormalization, but each will have a distinct type; in particular, if f is both w -renormalizable and w' -renormalizable (with $w \neq w'$), then w'_0 and w'_1 are finite words on symbols $\{w_0, w_1\}$ with at least one of each symbol, or vice versa. Defining $|w| = |w_0| + |w_1|$ we have that either $|w| < |w'|$, or $|w'| < |w|$ (Martens and de Melo, 2001).

Definition 1.11. Define the **renormalization operator**, \mathcal{R} , by sending a renormalizable f to the w -renormalization of f for which $|w|$ is minimal.

Maps for which $\mathcal{R}^j f$ is renormalizable for every $j \geq 0$ are called **infinitely renormalizable**; in the special case where $\mathcal{R}^j f$ is w -renormalizable and w does not depend on j , f is called **infinitely w -renormalizable** (this is also known by the name **stationary combinatorics**). The orbit $\{f, \mathcal{R}f, \mathcal{R}^2 f, \dots\}$ is called the **successive renormalizations** of f .

Conjecture 1.12. *The closure of the post-critical set, \mathcal{O}_f , of an infinitely w -renormalizable map f is a minimal Cantor attractor.*

Remark 1.13. For Lorenz maps, \mathcal{O}_f is the union of the ω -limit sets of the critical values, $f_0(c)$ and $f_1(c)$. This conjecture is a theorem for a large class of monotone combinatorics (Martens and Winckler, 2014; 2017).

1.3 Rigidity

Conjecture 1.14. *The set \mathcal{T}_w of infinitely w -renormalizable Lorenz maps coincides with the topological conjugacy class of any $f \in \mathcal{T}_w$. Furthermore, $\mathcal{T}_w \subset \mathcal{L}$ is a manifold of codimension two.*

Remark 1.15. The first statement would follow if it were shown that there are no wandering intervals for $f \in \mathcal{T}_w$. This is known for a large class of monotone combinatorics (Martens and Winckler, 2014; 2017) but the general problem of when Lorenz maps do not support wandering intervals is still wide open. The codimension of \mathcal{T}_w must be two since topologically full families of Lorenz maps are two-dimensional (Martens and de Melo, 2001).

Definition 1.16. The (classical) notion of **rigidity** is when two topologically conjugate maps are automatically smoothly conjugate on their attractors.

Remark 1.17. Smooth maps look affine on small scales, so in the presence of rigidity two maps have attractors which on a large scale may look very different but when zoomed in on a particular spot they start to look the same. In this sense rigidity is a strong form of **metric universality**; we will not say more about the latter here and instead focus on the former.

Remark 1.18. Two crucial ingredients in proving classical rigidity is first to prove that successive renormalizations converge and then to control the rate of convergence. Typically, these ingredients come from the fact that there is a hyperbolic renormalization fixed point which attracts both maps.

It is worth pointing out that the study of rigidity in dynamics was initiated by Herman (1979), answering a conjecture by Arnol'd (1961), but the close connection between rigidity and renormalization was only later realized.

Definition 1.19. The **rigidity class** of $f \in \mathcal{T}_w$ is defined as the set of $g \in \mathcal{T}_w$ such that f and g are smoothly conjugate on their attractors.

Remark 1.20. With this terminology we may characterize classical rigidity as the statement that a topological class coincides with a rigidity class. From [Martens and Winckler \(2017\)](#) we know that \mathcal{T}_w may, depending on w , consist of more than one rigidity class. Hence, the classical concept of rigidity is too restrictive, see also [Martens and Palmisano \(2017\)](#). Instead, the correct notion should be to describe the arrangement of a topological class into rigidity classes ([Martens et al., 2017](#)).

Even in the classical cases of critical circle maps and unimodal maps there is already a natural foliation into codimension-1 rigidity classes determined by a fixed value for the critical exponent. This is however a trivial observation compared to the above mentioned articles which concern far more subtle phenomena.

1.4 Main conjecture

Definition 1.21. The successive renormalizations of f are **attracted to a degenerate flipping 2-cycle** iff $\mathcal{R}^{2k}f$ and $\mathcal{R}^{2k+1}f$ converge to smooth maps on $[0, 1]$, and the critical points have limits $c(\mathcal{R}^{2k}f) \rightarrow 0$ and $c(\mathcal{R}^{2k+1}f) \rightarrow 1$ (or vice versa).

Remark 1.22. Here “degenerate” refers to the limits not being Lorenz maps and “flipping” refers to the fact that the critical points $c(\mathcal{R}^k f)$ flip between being close to zero and being close to one. Informally, the limiting cycle can be thought of as two Lorenz maps with critical point 0 and 1, respectively.

The Lorenz Renormalization Conjecture. Let \mathcal{T}_w be the set of infinitely w -renormalizable Lorenz maps. For each w (such that $\mathcal{T}_w \neq \emptyset$) exactly one of the following statements holds, and conversely, to each statement there are w for which it is realized:

- (A) \mathcal{T}_w is a rigidity class and the stable manifold of a hyperbolic renormalization fixed point.
- (B) \mathcal{T}_w is foliated by codimension-1 rigidity classes, one of which is the stable manifold of a hyperbolic renormalization fixed point. The successive renormalizations of any $f \in \mathcal{T}_w$ not in this stable manifold are attracted to a degenerate flipping 2-cycle.
- (C) There exists a nonempty, open and connected set $\mathcal{T}_w^* \subsetneq \mathcal{T}_w$ which is a rigidity class as well as the stable manifold of a hyperbolic renormalization fixed point; its complement, $\mathcal{T}_w \setminus \mathcal{T}_w^*$, consists of two connected components which are foliated by rigidity classes of codimension one. The boundary of \mathcal{T}_w^* in \mathcal{T}_w is a rigidity class as well as the stable manifold of a hyperbolic renormalization periodic point of (strict) period two. The successive renormalizations of any $f \in \mathcal{T}_w \setminus \mathcal{T}_w^*$ not in this stable manifold are attracted to a degenerate flipping 2-cycle.

Remark 1.23. The Lorenz Renormalization Conjecture can be generalized from stationary to periodic combinatorics in the obvious way. For unbounded combinatorics it is not clear what the right conjecture should be as it is possible to force successive renormalizations to not be relatively compact by choosing larger and larger return times for one branch. This leads to Lorenz maps whose attractor does not have a physical measure (Martens and Winckler, 2018).

Remark 1.24. A very surprising feature of Lorenz maps is that the dimension of the unstable manifold of a renormalization fixed point depends on the combinatorics; in cases (A) and (C) the dimension is two and in case (B) it is three. Two of the unstable directions are always related to moving the two critical values;³ a third unstable direction is gained when the movement of the critical point under renormalization becomes unstable (see figure 2). In the confounding case (C) there is a mix of both: the fixed point has two unstable directions, whereas the period-2 point has three unstable directions. This situation occurs e.g. for monotone (8, 2)-type (see figure 1).

Remark 1.25. Evidence for case (A) is supported by Martens and Winckler (2014). More recent is Martens and Winckler (2017) where the unstable behavior of the renormalization operator within topological classes was discovered; it supports case (B). Case (C) is so far only supported by this article. Numerically no other cases seem to occur, see § 2.6 for examples of each case.

Remark 1.26. Fixed points, f , of monotone (a, a) -type are symmetric⁴ and they are in one-to-one correspondence with unimodal renormalization fixed points; it is an exercise to verify that the unimodal map $g(x) = f(\min\{x, 1-x\})$, with $g(0.5) = 1$, is a fixed point of the unimodal renormalization operator. In particular, the monotone (1, 1)-type Lorenz renormalization fixed point corresponds to the well known fixed point of the unimodal period-doubling operator.

It seems reasonable to expect all of these “unimodal fixed points” to be dynamically similar, but curiously they are not; conjecturally, for $a > \max\{2\alpha - 1, 2\}$ they belong to case (B), else they belong to case (A). For example, when $\alpha = 2$ this “bifurcation” occurs for $a = 4$, see § 2.6.

Remark 1.27. Compare the Lorenz Renormalization Conjecture with the classical systems of unimodal maps, critical circle maps, etc. In these systems only case (A) can occur and the limit set of renormalization, \mathcal{A} , is a **horseshoe**; that is, \mathcal{A} is hyperbolic and the restriction $\mathcal{R}|_{\mathcal{A}}$ is conjugate to a full shift on infinitely many symbols. Furthermore, orbits of the renormalization operator (where defined) are exponentially contracted to \mathcal{A} (Avila and Lyubich, 2011).

As a counterpoint, the limit set of Lorenz renormalization cannot be a horseshoe due to case (C); instead, it seems to strictly contain a horseshoe which because of case (B) does not attract all orbits of renormalization.

Remark 1.28. Consider how the Lorenz Renormalization Conjecture influences **parameter universality** phenomena.

³Just as the one unstable direction for unimodal renormalization is related to moving the one critical value.

⁴That is, the critical point is $c(f) = 0.5$ and $1 - f(x) = f(1 - x)$.

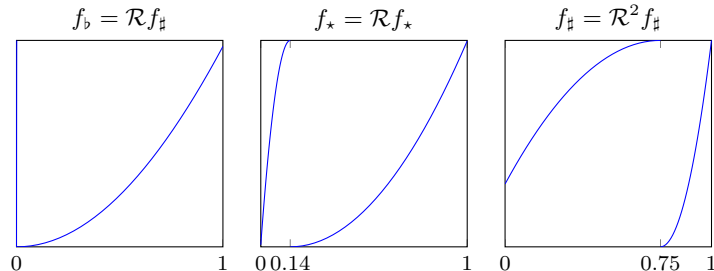


Figure 1: The fixed point f_* and period-2 orbit $\{f_b, f_\#\}$ of monotone $(8, 2)$ -type. Note that f_b appears to only have one branch because its critical point is very close to zero, $c(f_b) \approx 0.0013$.

Classically, a topologically full family (of dimension one) transversally intersects a stable manifold (of codimension one) of a hyperbolic renormalization fixed point; this causes iterated images of the family under renormalization to accumulate on an unstable manifold and the bifurcation patterns of the family asymptotically look like those of the unstable manifold.

Here, the iterated images of a topologically full family (which has dimension two) under renormalization need not accumulate on an unstable manifold; it depends on which rigidity class the family hits (a stable manifold may have codimension three inside \mathcal{L}). However, a three-dimensional family will generically hit all rigidity classes and hence asymptotically contain all possible bifurcation patterns. Universality persists but in a more intricate fashion and there is now a distinction between topologically full families (of dimension two) and geometrically full families (of dimension three).

2 Numerics

In this section numerical experiments which support the Lorenz Renormalization Conjecture are described.

The purpose of these experiments is to locate approximate renormalization fixed points and to estimate the relative sizes of the eigenvalues of the derivative of \mathcal{R} at these fixed points. Approximate periodic points of \mathcal{R} can also be located with this method by considering the combinatorics of twice renormalizable maps. The purpose is *not* to provide accurate estimates.

This method will not rule out existence of other periodic points of renormalization, only to give evidence in favor of existence of the three cases of the Lorenz Renormalization Conjecture. From our observations there seem to be no other cases.

2.1 Representation of Lorenz maps

Definition 2.1. Let \mathcal{D} denote the set of orientation-preserving diffeomorphisms on $[0, 1]$ and define the family

$$F : (0, 1) \times [0, 1] \times (0, 1] \times \mathcal{D} \times \mathcal{D} \rightarrow \mathcal{L}$$

as follows: given (c, v, ϕ) , where $v = (v_0, v_1)$ and $\phi = (\phi_0, \phi_1)$, define $F(c, v, \phi)$ to be the Lorenz map $f : [0, 1] \setminus \{c\} \rightarrow [0, 1]$ whose branches $f_0 : [0, c] \rightarrow [v_0, 1]$ and $f_1 : [c, 1] \rightarrow [0, v_1]$ are the rescalings of $\phi_0(1 - (1 - x)^\alpha)$ and $\phi_1(x^\alpha)$, respectively (see definition 1.7). The parameters $v = (v_0, v_1)$ are called **boundary values**.

Remark 2.2. It is clear that F is injective; furthermore, its image is renormalization invariant by lemma 2.5.

Definition 2.3. Let $D \subset \mathcal{D}$ be a finite-dimensional subset of diffeomorphisms together with a projection $\text{proj}_D : \mathcal{D} \rightarrow D$. Let

$$L = (0, 1) \times [0, 1] \times (0, 1] \times D \times D$$

denote the **set of truncated Lorenz maps**.

Remark 2.4. For simplicity of implementation, we choose D to be a set of piecewise linear homeomorphisms. Of course, this is not a subset of diffeomorphisms but for the purpose of the numerics it empirically does not matter.

To address the issue of smoothness, cubic interpolation could be used instead of linear interpolation, but then care has to be taken that the interpolation is monotone. Another idea is to linearly interpolate functions on $[0, 1]$ and taking the inverse of the nonlinearity operator; this would ensure monotonicity as well as C^2 -smoothness. A third idea is to use finite pure internal structures, which ensures monotonicity and C^∞ -smoothness (Martens and Winckler, 2014).

We choose not to pursue these paths here as the implementation would become more involved and since it would not give qualitatively different results.

2.2 Truncated renormalization

Lemma 2.5. Let $f = F(c, v, \phi)$ as in definition 2.1. If f is w -renormalizable, then $\mathcal{R}f = F(c', v', \phi')$ for some (c', v', ϕ') . Explicitly, let $n_k = |w_k|$, $p_0 = f^{n_0-1}(0)$, $p_1 = f^{n_0-1}(1)$, $\tilde{\phi}_0(x) = v_0 + (1 - v_0)\phi_0(x)$, and $\tilde{\phi}_1(x) = v_1\phi_1(x)$; then

$$c' = \frac{c - p_0}{p_1 - p_0}, \quad v'_0 = \frac{f^{n_0}(p_0) - p_0}{p_1 - p_0}, \quad v'_1 = \frac{f^{n_1}(p_1) - p_0}{p_1 - p_0}, \quad (1)$$

and ϕ'_0, ϕ'_1 are the respective rescalings of

$$\begin{aligned} f^{n_0-1} \circ \tilde{\phi}_0 &: [\tilde{\phi}_0^{-1} \circ f(p_0), 1] \rightarrow [f^{n_0}(p_0), p_1], \\ f^{n_1-1} \circ \tilde{\phi}_1 &: [0, \tilde{\phi}_1^{-1} \circ f(p_1)] \rightarrow [p_0, f^{n_1}(p_1)]. \end{aligned}$$

Proof. Denote the first-return map associated with the renormalization by $g : I \setminus \{c\} \rightarrow I$, where $I = [p_0, p_1]$. Then c' is the relative position of c in I , v'_0 is the relative length of $g([p_0, c])$ in I , and v'_1 is the relative length of $g((c, p_1])$ in I ; written out this is (1). The statement for ϕ'_0, ϕ'_1 is just saying that they are the branches of g without the initial folding x^α that comes from $f|_I$. Since g is a first-return to I the f -images of I do not meet the critical point before they return; this means that ϕ'_k are diffeomorphisms. \square

Definition 2.6. Let F and (D, proj_D) be as in definitions 2.1 and 2.3, respectively, and let $P(c, v, \phi) = (c, v, \text{proj}_D(\phi_0), \text{proj}_D(\phi_1))$. For every renormalizable $F(c, v, \phi)$, define the **truncated renormalization operator**, R , by

$$R(c, v, \phi) = P \circ F^{-1} \circ \mathcal{R} \circ F(c, v, \phi).$$

This is well-defined by remark 2.2.

Remark 2.7. For a class of monotone combinatorics with $|w|$ large the renormalization operator is close to having finite dimensional image, in the sense that the diffeomorphisms ϕ'_k in lemma 2.5 are close to being linear (Martens and Winckler, 2017). In other words, R can automatically be a good approximation of \mathcal{R} , depending on the combinatorics.

Remark 2.8. Taking the above remark to its extreme, it even makes sense to consider the trivial set $D = \{\text{id}\}$ of diffeomorphisms, and looking at the corresponding truncated renormalization operator; it is explicitly defined by (1) with $\phi = (\text{id}, \text{id})$. This is the operator we used to estimate the eigenvalues in figure 2.

Empirically, it exhibits all the dynamics of the Lorenz Renormalization Conjecture and seems to be a remarkably good approximation of the full renormalization operator as far as qualitative behavior is concerned. This should not come as a great surprise as one method of proving existence of fixed points for \mathcal{R} involves homotoping to this three-dimensional truncation and proving it has a fixed point (Martens and Winckler, 2014; 2017).

Definition 2.9. For every renormalizable $F(c, v, \phi)$, define the **modified renormalization operator**, $\tilde{R} : (c, v, \phi) \mapsto (c', v')$, in the same way as the truncated renormalization operator, except changing (1) to

$$\begin{aligned} c' &= p_0 - c + (p_1 - p_0)c, \\ v'_0 &= p_0 - f^{n_0}(p_0) + (p_1 - p_0)v_0, \\ v'_1 &= p_0 - f^{n_1}(p_1) + (p_1 - p_1)v_1. \end{aligned}$$

Note that the image of \tilde{R} is contained in \mathbb{R}^3 .

Remark 2.10. The idea of the above operator is to improve the numerical behavior of R by not dividing by the length of the return interval in (1). From the same equation it can be seen that the set of zeros of \tilde{R} coincide with the set of (c, v, ϕ) for which (c, v) are fixed by R . We found that the Newton method on \tilde{R} has better convergence properties than the Newton method on $R - \text{id}$. Given w , we use it to determine what the right value for c should be for a truncated renormalization fixed point (see the fixed point algorithm in the next section).

2.3 Locating fixed points

The perhaps simplest idea for locating fixed points of the truncated renormalization operator is to use a Newton iteration. This is feasible for short combinatorics, but for longer combinatorics it is practically impossible to find starting guesses for which it converges.

The method we employ can be thought of as acting on the two-dimensional families $v \mapsto F(c, v, \phi)$ (see definition 2.1). It consists of three separate algorithms: one which determines a v such that $F(c, v, \phi)$ is renormalizable, followed either by an algorithm which takes $F(c, v, \phi)$ and produces a new c , or one which takes $F(c, v, \phi)$ and produces a new ϕ . Combined, these methods empirically behave like a contraction toward a family which contains a renormalization fixed point and for which the first algorithm is a contraction toward this fixed point.

Definition 2.11 (Renormalization fixed point algorithm). Input: the combinatorics w .

- (1) Pick an initial guess for c and ϕ .
- (2) Apply the modified Thurston algorithm to $v \mapsto F(c, v, \phi)$ to get new boundary values v' (see § 2.4 and remark 2.15).
- (3) Take a Newton step with the operator \tilde{R} on $F(c, v', \phi)$ to get a new critical point c' .
- (4) Apply the modified Thurston algorithm to $v \mapsto F(c', v, \phi)$ to get new boundary values v'' .
- (5) Apply R to $F(c', v'', \phi)$ to get new diffeomorphisms ϕ' .
- (6) Stop if $(c, v, \phi) = (c', v'', \phi')$, else set $c = c'$, $\phi = \phi'$ and go back to step (2).

Output: the Lorenz map $F(c, v, \phi)$ (supposedly a renormalization fixed point).

Remark 2.12. The above algorithm empirically seems to converge for the initial guesses $\phi = (\text{id}, \text{id})$ and a large set of c . Theoretically, there is no guarantee for the output to be a renormalization fixed point, but practically we observe that it is (as long as the algorithm converges).

2.4 The Thurston algorithm

The Thurston algorithm is a fixed point method that realizes any periodic combinatorics in a full family of maps. It originates in Douady and Hubbard (1993) and is also known as the Spider Algorithm in the complex setting (Hubbard and Schleicher, 1994). In real dynamics it is usually employed to prove the full family theorem (Martens and de Melo, 2001; de Melo and van Strien, 1993). We use it to locate renormalizable maps within the two-dimensional families $v \mapsto F(c, v, \phi)$ (see definition 2.1).

Definition 2.13 (The Thurston Algorithm). Input: a critical point c , diffeomorphisms $\phi = (\phi_0, \phi_1)$, and combinatorics $w = (w_0, w_1)$.

- (1) Pick an initial guess of **shadow orbits**⁵

$$\{x_k(0) = k, x_k(1), \dots, x_k(m-1) = c\}, \quad m = |w_0| + |w_1|, \quad k = 0, 1.$$

Let W_k be the concatenation of w_k followed by w_{1-k} , for $k = 0, 1$.

- (2) Set $v = (x_0(1), x_1(1))$, and let $f = F(c, v, \phi)$ with branches f_0 and f_1 .
(3) Pull back x_k with f according to the combinatorics W_k :

$$y_k(j-1) = f_{W_k(j)}^{-1}(x_k(j)), \quad j = 1, \dots, m-1, \quad k = 0, 1.$$

- (4) Set $y_k(m-1) = c$, $k = 0, 1$.

- (5) Stop if $y_k = x_k$, else set x_k to y_k , $k = 0, 1$, and go back to (2).

Output: the map f which is a realization of the combinatorics w in the family $v \mapsto F(c, v, \phi)$.

Remark 2.14. As long as the initial guess is chosen consistently (i.e. if the shadow orbits are ordered according to w) this algorithm is guaranteed to stop; in this case, the realization f is renormalizable and the boundary values of Rf equal the critical point of Rf .

In practice the algorithm converges if the initial guess consists of uniformly spaced points $x_0(0) < \dots < x_0(m-1)$ and $x_1(0) > \dots > x_1(m-1)$ even though these are not ordered according to the combinatorics w .

Remark 2.15. We modify the above algorithm so that the realization f fixes its boundary values under renormalization; i.e. $Rf(k) = f(k)$, for $k = 0, 1$. This is convenient as we are interested in renormalization fixed points. The modification is to replace step (4) with:

- (4') Let $p_0 = x_0(|w_1| - 1)$ and $p_1 = x_1(|w_0| - 1)$ and set

$$y_k(m-1) = p_0 + (p_1 - p_0)v_k, \quad k = 0, 1.$$

Note that $[p_0, p_1]$ is the return interval of f if $y_k = x_k$, so what this step does is to set the relative boundary values of the first-return map. Replacing v_k with parameters t_k varying in $[0, 1]$ it is possible to find the whole domain of w -renormalizability in the family.

Remark 2.16. There is a relationship between the modified Thurston algorithm from the previous remark and the renormalization operator—if the modified Thurston algorithm is applied to a family which contains a renormalization fixed point then the output of the algorithm will be the renormalization fixed point. So the renormalization fixed point is also the fixed point of a contractive “Thurston operator.”

⁵The name comes from the fact that in the end x_k will be actual orbits of the critical values 0 and 1 under some map f in the family; i.e. $x_k(j) = f^j(k)$.

2.5 Implementation

The source code for an implementation of the fixed point algorithm of § 2.3 is freely available online (Winckler, 2018). It compiles to three executables which were used to produce the results of § 2.6; see the accompanying README for instructions on how to reproduce the results.

The Eigen library (Guennebaud and Jacob, 2010) is used for linear equation solvers and eigenvalue estimation; we also use its bindings to the multiple precision library MPFR (Fousse et al., 2007; Holoborodko, 2008) as well as its automatic differentiation routines. Standard double precision arithmetic is only sufficient for short combinatorics, which is why the implementation needs multiple precision. Automatic differentiation is used to evaluate the derivative of R . Note that this is not the same thing as numerical differentiation (taking finite differences); instead it uses the chain-rule to exactly (up to numerical precision) evaluate derivatives.

2.6 Results

The experiments in this section were performed using a truncation of R in dimension three up to dimension 1000. Higher dimensions were needed only when evaluating the renormalization of period-2 points, such as in figure 1, otherwise the three-dimensional truncation gave qualitatively accurate results. Results are only stated for monotone combinatorics; some non-monotone combinatorics were tested as well but it is harder to present these in a clear manner so they are not included. The programs also work with arbitrary α but experiments investigating the α -dependence have been left out to keep this section focused.

The following table shows which of case (A), (B) or (C) of the Lorenz Renormalization Conjecture the first few monotone (a, b) -types fall under for $\alpha = 2$:

1	2	3	4	5	6	7	8	9	\dots	(a, b)
A	A	A	A	A	A	A	A	A	\dots	1
	A	A	A	A	A	C	C	C	\dots	2
		A	B	B	B	B	B	B	\dots	3
			B	B	B	B	B	B	\dots	4
				B	B	B	B	B	\dots	5
					B	B	B	B	\dots	6
						B	B	B	\dots	7
							B	B	\dots	8
								B	\dots	9

For example, the above table shows that (a, a) -type has a two-dimensional unstable manifold for $a = 1, 2, 3$, and a three-dimensional unstable manifold for $a \geq 4$; $(a, 2)$ -types with $a \geq 7$ has both a fixed point and a period-2 point. Note that the complete table is symmetric about the diagonal.

Remark 2.17. It is known that a and b sufficiently large implies case (B) (Martens and Winckler, 2017). It is not clear exactly when case (C) occurs; from the above table only $(a, 1)$ -type and $(a, 2)$ -type seem viable, but a test with increasing a did not reveal any $(a, 1)$ -types of case (C). Note that we are only discussing stationary combinatorics and $\alpha = 2$ here.

In creating the above table we performed roughly the following steps:

- (1) Locate a fixed point for the three-dimensional truncated renormalization operator (see remark 2.8), using $c = 0.5$ as an initial guess for the critical point; if it doesn't converge, try other values for c until it does.

The derivative of the three-dimensional truncation of R at the fixed point has three eigenvalues. Denote the eigenvalue with the smallest magnitude by λ_c ; this is the eigenvalue associated with moving the critical point (the other two eigenvalues are associated with changing the boundary values). If $\lambda_c \in (0, 1)$ then we must be in case (A); if $\lambda_c \in (-1, 0]$ we go to the next step; if $|\lambda_c| > 1$ we must be in case (B). The behavior of λ_c is illustrated in figure 2.

- (2) Try to locate a period-2 orbit of R by looking for a fixed point of twice (a, b) -renormalizable type.⁶ We observe in this situation that one of three things happen:
 - (i) the algorithm diverges by $c \uparrow 1$ (most common case),
 - (ii) the algorithm converges to the fixed point found in the previous step (only seems to happen if c is picked close to the c of the fixed point),
 - (iii) the algorithm converges and c is different from that of the fixed point.

In the first two situations we are in case (A) and in the last situation we are in case (C). In the first two situations this step is repeated with different guesses for c to make sure the last situation was not missed due to a bad initial guess.

The graphs of the fixed point and period-2 orbit for $(8, 2)$ -type can be found in figure 1.

- (3) Increase the dimension of the truncation of R to see if it affects the above classification; in all cases we tried the eigenvalues changed slightly in value but not enough to affect the classification.

⁶For example, once $(2, 1)$ -renormalizable type is given by $(011, 10)$ and twice $(2, 1)$ -renormalizable is given by $(0111010, 10011)$.

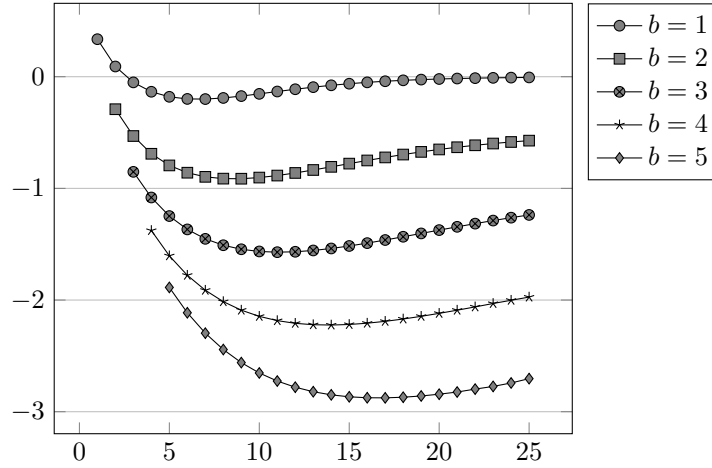


Figure 2: Dependence of the eigenvalue associated with movement of the critical point on monotone type (a, b) for $\alpha = 2$; estimated using the three-dimensional truncation of R .

Notation

f, f_0, f_1	Lorenz map f with branches f_0, f_1	2
$c, c(f)$	the critical point of f	2
α	critical exponent	2
\mathcal{L}	set of Lorenz maps	2
$w = (w_0, w_1)$	type of renormalization	3
\mathcal{R}	renormalization operator	4
\mathcal{T}_w	topological class	4
$v = (v_0, v_1)$	boundary values, $v_k = f(k)$	8
$\phi = (\phi_0, \phi_1)$	diffeomorphisms	8
F	family of Lorenz maps $F(c, v, \phi)$	8
D, proj_D	finite-dimensional diffeomorphism, projection	8
L	set of truncated Lorenz maps	8
R, \tilde{R}	truncated renormalization operators	9, 9

References

- Arneodo, A., P. Coulet, and C. Tresser. 1981. *A possible new mechanism for the onset of turbulence*, Phys. Lett. A **81**, no. 4, 197–201.
- Arnol'd, V. I. 1961. *Small denominators. I. Mapping the circle onto itself*, Izv. Akad. Nauk SSSR Ser. Mat. **25**, 21–86.
- Avila, A. and M. Lyubich. 2011. *The full renormalization horseshoe for unimodal maps of higher degree: exponential contraction along hybrid classes*, Publ. Math. Inst. Hautes Études Sci. **114**, 171–223.
- De Carvalho, A., M. Lyubich, and M. Martens. 2005. *Renormalization in the Hénon family. I. Universality but non-rigidity*, J. Stat. Phys. **121**, no. 5-6, 611–669.

- Chandramouli, V. V. M. S., M. Martens, W. de Melo, and C. P. Tresser. 2009. *Chaotic period doubling*, Ergod. Theory Dyn. Syst. **29**, no. 2, 381–418.
- Collet, P., J.-P. Eckmann, and H. Koch. 1981. *Period doubling bifurcations for families of maps on \mathbf{R}^n* , J. Statist. Phys. **25**, no. 1, 1–14.
- Couillet, P. and C. Tresser. 1978. *Itérations d'endomorphismes et groupe de renormalisation*, C. R. Acad. Sci. Paris Sér. A-B **287**, no. 7, A577–A580.
- Douady, A. and J. H. Hubbard. 1993. *A proof of Thurston's topological characterization of rational functions*, Acta Math. **171**, 263–297.
- Eckmann, J.-P., H. Koch, and P. Wittwer. 1984. *A computer-assisted proof of universality for area-preserving maps*, Mem. Amer. Math. Soc. **47**, no. 289, vi+122.
- Fousse, L., G. Hanrot, V. Lefèvre, P. Pélissier, and P. Zimmermann. 2007. *MPFR: A Multiple-precision Binary Floating-point Library with Correct Rounding*, ACM Trans. Math. Softw. **33**, no. 2.
- Gaidashev, D., T. Johnson, and M. Martens. 2016. *Rigidity for infinitely renormalizable area-preserving maps*, Duke Math. J. **165**, no. 1, 129–159.
- Guckenheimer, J. and R. F. Williams. 1979. *Structural stability of Lorenz attractors*, Inst. Hautes Études Sci. Publ. Math. **50**, 59–72.
- Guennebaud, G. and B. Jacob. 2010. *Eigen v3*. available at <http://eigen.tuxfamily.org>.
- Herman, M. 1979. *Sur la conjugaison différentiable des difféomorphismes du cercle à des rotations*, Inst. Hautes Études Sci. Publ. Math. **49**, 5–233.
- Hirsch, M. W., C. C. Pugh, and M. Shub. 1977. *Invariant manifolds*, Lecture Notes in Mathematics, Vol. 583, Springer-Verlag, Berlin-New York.
- Holoborodko, P. 2008. *MPFR C++*. available at <http://www.holoborodko.com/pavel/mpfr/>.
- Hubbard, J. H. and D. Schleicher. 1994. *The spider algorithm*, Proc. Sympos. Appl. Math., vol. 49, Amer. Math. Soc., Providence, RI.
- Khanin, K. and A. Teplinsky. 2013. *Renormalization horseshoe and rigidity for circle diffeomorphisms with breaks*, Comm. Math. Phys. **320**, no. 2, 347–377.
- Linsay, P. S. 1981. *Period doubling and chaotic behavior in a driven anharmonic oscillator*, Phys. Rev. Lett. **47**, no. 19, 1349–1352.
- Lorenz, E. N. 1963. *Deterministic nonperiodic flow*, J. Atmospheric Sci. **20**, 130–141.
- Martens, M. and W. de Melo. 2001. *Universal models for Lorenz maps*, Ergod. Theory Dyn. Syst. **21**, no. 3, 833–860.
- Martens, M. and L. Palmisano. 2017. *Rigidity foliations*, available at [arXiv:1704.06328](https://arxiv.org/abs/1704.06328).
- Martens, M., L. Palmisano, and B. Winckler. 2017. *The rigidity conjecture*, Indagationes Mathematicae, DOI 10.1016/j.indag.2017.08.001.
- Martens, M. and B. Winckler. 2014. *On the hyperbolicity of Lorenz renormalization*, Comm. Math. Phys. **325**, no. 1, 185–257.
- Martens, M. and B. Winckler. 2017. *Instability of Renormalization*, available at [arXiv:1609.04473](https://arxiv.org/abs/1609.04473).
- . 2018. *Physical measures for infinitely renormalizable Lorenz maps*, Ergod. Theory Dyn. Syst. **38**, no. 2, 717–738.
- Maurer, J. and A. Libchaber. 1979. *Rayleigh–Bénard experiment in liquid helium; frequency locking and the onset of turbulence*, J. de Phys. Lett. **40**, no. 16, 419–423.
- de Melo, W. and S. van Strien. 1993. *One-dimensional dynamics*, Vol. 25, Springer-Verlag, Berlin.
- Milnor, J. 1997. *Fubini Foiled: Katok's Paradoxical Example in Measure Theory*, Math. Intelligencer **19**, no. 2, 30–32.
- Winckler, B. 2018. *The Lorenz Renormalization Conjecture – supplementary material*. available at <https://github.com/b4winckler/src-lorenz-renorm-conj>.
- Yampolsky, M. 2003. *Renormalization horseshoe for critical circle maps*, Comm. Math. Phys. **240**, no. 1-2, 75–96.